AN OVERVIEW OF RECENT LABORATORY MEASUREMENTS ON DISPERSION AND ATTENUATION IN BUBBLY LIQUIDS, AND SCATTERING FROM ARTIFICIAL BUBBLE CLOUDS

PRESTON S. WILSON

The University of Texas at Austin, Mechanical Engineering Department
1 University Station C2200, Austin, TX 78712, USA
E-mail: pswilson@mail.utexas.edu

RONALD A. ROY

Boston University, Department of Aerospace and Mechanical Engineering
110 Cummington Street, Boston, MA, 02115, USA
E-mail: ronroy@bu.edu

Effective medium (EM) models are commonly used to describe the acoustics of bubbly liquids. Regarding linear sound propagation, this approach has been successful for low void fractions and broad bubble size distributions, at frequencies away from the individual bubble resonance frequency (IBRF). For narrow size distributions at frequencies near IBRF, previously reported sound speed and attenuation measurements are not well-described by EM models. Due to high attenuation in the medium and the difficulty of independently characterizing bubble populations, experimental verification of competing models has not been achieved. An impedance tube technique was developed to overcome these difficulties and used to investigate narrow bubble size distributions at IBRF. Agreement with existing theory to a greater degree than previously reported was observed up to a void fraction of 5.4×10^{-4}, within the uncertainty of the bubble population parameters. Regarding free-field scattering from clouds of freely rising bubbles, EM models have typically been found effective up to the cloud's monopole resonance frequency. Measurements of scattering from bubble collections that had a well-defined shape were conducted. An EM scattering model was found to describe the measurements at frequencies up to three times the cloud's monopole resonance frequency and up to 55% of the mean bubble resonance frequency.

1 Introduction

Bubbles and bubble clouds near the ocean surface add greatly to the complexity of shallow water acoustics, but as recently as 1965, a standard textbook in underwater acoustics stated that large numbers of bubbles did not occur regularly in the ocean, except in the wakes of ships [1]. It is now well known that the upper layers of the ocean can contain as many as 10^6 bubbles per cubic meter, even in calm seas [2]. Supersaturation of sea water by spring warming, snow, rain, and wave breaking are all known to produce bubbles at or near the surface [3]. In addition, marine plant photosynthesis, decomposition of organic material, and geological processes contribute to the continual presence of bubbles throughout the water column [2]. Perhaps the most

N.G.Pace and P Blondel, (Eds), Boundary Influences In High Frequency, Shallow Water Acoustics Pages 441-448, University of Bath, UK 5th-9th September 2005

acoustically relevant bubbles are those produced by spilling and plunging breakers, which can form into plumes and clouds [4] and can migrate, via turbulence [5] and Langmuir currents [6], into a variety of spatial distributions and be transported to depths as great as 30 meters. These bubble clouds can cause attenuation as high as 60 dB per meter [2] and persist for minutes at a time [4]. Measurements have shown that bubble clouds have high target strengths, of order −1 dB [7, 8]. In addition to these naturally occurring bubbles, highly organized and persistent bubbles are also found in the wakes of ships. Bubbles and bubble clouds also generate noise [9], and exhibit strong nonlinear effects [10, 11].

Sound propagation below IBRF, and sound propagation at and above IBRF, through bubbles with a broad bubble size distribution (BSD) and void fractions below about 10^{-4}, is fairly well understood [12]. Propagation through narrow size distributions of bubbles excited near IBRF and at higher void fractions is not well understood [12-14]. The high attenuation, of order 10 dB/cm in this regime, and the difficulty in obtaining bubble size measurements of sufficient accuracy has left competing models unverified by experiment [13, 14]. Due to the complex shape of natural bubble clouds, and the difficulty of independently monitoring cloud size, shape and bubble content, there is an absence of single-cloud scattering data suitable for systematic model comparison above the cloud's monopole resonance frequency [8].

In this paper, we review recent laboratory scattering and propagation experiments [15, 16] that were conducted on well-characterized bubble populations in order to facilitate meaningful model comparison with a minimum of fitted parameters. The measurements were found to compare favorably to existing effective-medium propagation and scattering models. The propagation experiments focused on frequencies near IBRF and show increased model agreement compared to previously reported data [12]. The frequency range of the scattering experiments was sub-IBRF, but in the resonance regime associated with collective oscillation of the bubble cloud. Some of the scattering experiments show better model agreement than one might expect, given the limitations of the effective medium model that was used.

2 Propagation Measurements: Sound Speed and Attenuation

2.1 Description of the Experiment

Near IBRF, high attenuation prohibits time-of-flight and standing wave measurements, so an impedance tube technique was used [17]. Frequency-dependent sound speed and attenuation within the bubbly liquid were inferred from measurements of the effective plane wave specific acoustic impedance z_s at the surface of the bubbly liquid. The experiments reviewed here are described in detail elsewhere [16], but an overview of the apparatus and procedure are given.

A schematic diagram of the impedance tube system is shown in Figure 1. The bubbles were generated directly at the measurement plane of the impedance tube, by either a single needle, which was lowered down into the impedance tube, or with a bubble injection manifold (BIM) that fit inside the impedance tube and deployed multiple needles. The needle and the BIM can be moved between the impedance tube and two other systems (not shown in Figure 1) that were used to determine the BSD and

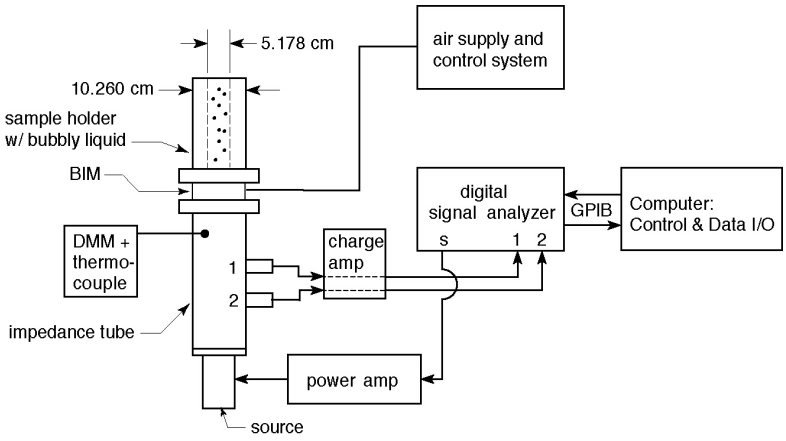

Figure 1. A schematic diagram of the impedance tube system is shown.

the void fraction. The experimental procedure was composed of four parts. First, the impedance tube was the calibrated. The needle or BIM was then installed in an optical apparatus for the measurement of the BSD. For needle-generated bubbles, void fraction was also measured in the optical apparatus. For BIM-generated bubbles, the BIM was moved to a third apparatus for void fraction measurement. Finally, the needle or BIM was installed in the impedance tube and the surface impedance z_s of the bubble layer was measured.

Impedance tube construction, calibration and operation have been described previously [17]. Briefly, the system consists of a thick-walled stainless steel tube with two custom fabricated wall-mounted hydrophones. The system was designed to admit waves that are plane (to a high degree of approximation), despite some coupling between the fill-material and the tube wall. The acoustic source was a Kildare Corporation TP-400/A tonpilz. The bubbly liquid was contained within a sample holder. Pseudo-random noise signals were generated and received with a Hewlett-Packard HP89410A vector signal analyzer. A Crown CE-1000 amplified the excitation signal and the hydrophone signals were conditioned with a charge amplifier. The transfer function between the two hydrophones was measured with the HP89410A and the data were transferred to a laptop computer for storage and processing. The surface impedance z_s of the bubbly liquid is related to the measured transfer function using Eq. (1) of [17], and a set of calibration functions. High attenuation prevented surface reflections from the top of the bubbly layer, hence $z_s = \rho c_m$. The bubbly mixture density ρ was known and phase speed and attenuation were obtained from c_m.

2.2 The Propagation Model

The measurements are compared to a model for linear sound propagation put forth by Commander and Prosperetti [12]. For circular excitation frequency ω, the complex sound speed in the bubbly mixture c_m is given by

$$\frac{c_l^2}{c_m^2} = 1 + 4\pi c_l^2 \int_0^\infty \frac{ap(a)da}{\omega_0^2 - \omega^2 + 2ib\omega}, \tag{1}$$

where the host liquid has sound speed c_l , density ρ_l, viscosity μ, surface tension σ and equilibrium pressure P_∞. The number of bubbles per unit volume with equilibrium radius between a and $a + da$ is $p(a)da$. The bubbles have equilibrium internal bubble pressure $P_{b,e} = P_\infty + 2\sigma/a$, and damping coefficient

$$b = \frac{2\mu}{\rho_l a^2} + \frac{P_{be}}{2\rho_l a^2 \omega} \mathrm{Im}\Phi + \frac{\omega^2 a}{2c_l}. \tag{2}$$

The three terms are due to viscous, thermal and acoustic dissipation effects, respectively. The terms Φ and ω_0 are defined in [12] and relate to the gas thermal behavior and the bubble resonance frequency, respectively.

The comparison between sound speed and attenuation measured with the impedance tube and the predictions of Eq. (1) are presented for a number of void fractions in Figure 2. A complete description of the data analysis is beyond the present scope but is discussed elsewhere [16]. The dominant source of uncertainty in the entire experiment is with the probability distribution function $p(a)$, and is due directly to uncertainty in individual bubble radius (+/– 10%), the finite number of bubble observations, and

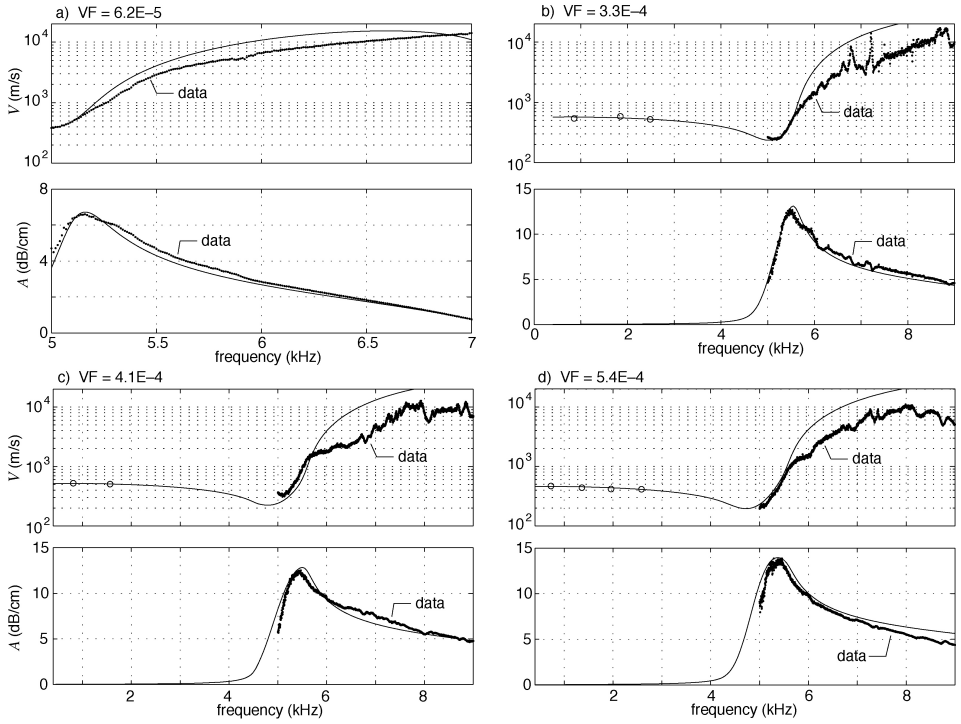

Figure 2. Model/data comparison for sound propagation in bubbly liquid at four void fractions. In each of the sub-figures a) through d), the upper frame is phase speed V (m/s) and the lower frame is attenuation A (dB/cm). In a), a single needle was used to produce the bubbles, otherwise the BIM was used. The large open circles represent data obtained from the void fraction resonator.

instability in the bubble production system (which led to non-stationary population statistics). For a given void fraction, a truncated normal distribution was fit to the observed bubble size measurements and a predicted sound speed and attenuation was calculated. Some of the statistical distribution parameters, such as mean bubble radius and standard deviation, where then adjusted to best fit the measured attenuation curve. This adjustment was well within the range of the bubble size measurement uncertainty itself. Void fraction was not adjusted. The best-fit bubble population statistics that were used in the model predictions are shown in Table 1.

Good agreement near IBRF is seen in all cases. The predicted and measured peak attenuation are within 1 dB and the shape of the measured and predicted attenuation curves are very similar. There is a deviation between measured and predicted phase speed above IBRF. At and below IBRF, the bubbly liquid is acoustically soft compared to the walls of the impedance tube, but above IBRF, as the phase speed increases, the bubbly liquid becomes acoustically hard compared to the walls. This causes elastic waveguide effects to become prominent, one of which is a reduced phase speed relative to the unconfined value. Therefore, the phase speed measured in the impedance tube, is reduced relative to the free field value predicted by Eq. (1). This effect is expected and is further discussed in [16]. Near IBRF though, elastic waveguide effects are at a minimum, and the data shown in Figure 2 are consistent with behavior in the free field.

Table 1. The bubble population statistics used to form $p(a)$ in Eq (1), as plotted in Figure 2. A truncated normal distribution was used, described by the population minimum, mean and maximum bubble radii, and the population standard deviation, respectively.

void fraction, VF	$a_{\min}$ (mm)	a_0 (mm)	$a_{\max}$ (mm)	s (mm)
6.2×10^{-5}	0.627	0.636	0.645	0.005
3.3×10^{-4}	0.58	0.60	0.75	0.031
4.1×10^{-4}	0.58	0.62	0.71	0.038
5.4×10^{-4}	0.58	0.64	0.75	0.035

3 Scattering from Artificial Bubble Clouds of Canonical Shape: Bubbly-Liquid-Filled Compliant Cylinders

Obtaining knowledge and control of naturally occurring bubble cloud shape, size and bubble content with sufficient accuracy for systematic investigation of scattering properties, including comparison with model predictions, has not been achieved. Monopole scattering from artificially generated, acoustically compact bubble clouds has been investigated [8]. For excitation frequencies well below IBRF, such clouds scatter sound as if they were effective fluid spheres, with effective density and sound speed given by Wood's mixture rule [18]. Above the monopole resonance frequency, these clouds were not acoustically compact and did not exhibit fluid-sphere scattering. To extend the frequency range of investigation, clouds of canonical shape were used. Thin-walled rubber tubes provided both a means to be filled with bubbly liquid, and a structure for which the scattering formulation was known.

3.1 Description of the Experiment

The experiments were conducted in a large indoor tank. A 3-m length of thin-walled latex-rubber tubing was deployed horizontally in the tank and served as the scattering target. A bubbly fluid generator (BFG), described in [15], was used to produce a large volume of microbubble-filled liquid that could be pumped through a closed fluid circuit that contained the target. Void fraction was monitored above the tank's water surface, several meters down-line from the target; not to determine absolute void fraction, but to verify that the void fraction remained constant throughout the experiment. BSD was also measured down-line, with a flow-through photographic imaging cell. Void fraction and BSD directly within the target was not monitored. Time-resolved incident and reflected acoustic pulses were recorded for a range of frequencies and two tube sizes, and echo level was determined from the measured acoustic pulses. A complete description of the measurement procedure and data processing is given in [15]. Results for the larger of the two tube sizes over a frequency range from 5–20 kHz have already been reported [15]. Results for the smaller tube and an extended frequency range are reported here.

3.2 Overview of the Scattering Model

The majority of the bubbles produced by the BFG were below resonance size for the experimental excitation frequencies and Wood's equation [18] was used to describe the sound speed and density of the bubbly liquid within the tube. Doolittle and Überall's scattering formulation [19] for an elastic-walled, fluid-filled cylindrical shell was then used to predict the amplitude of the scattered wave

$$P_{\mathrm{sc}} = P_0 \sum_{m=0}^{\infty} A_m H_m^{(1)}(kr)\cos(m\theta), \tag{3}$$

where P_0 is pressure amplitude of the incident wave, and A_{m} are determined from the boundary conditions, geometry and material properties, including those of the bubbly liquid. $H_m^{(1)}$ is an m-th order Hankel function of the first kind and k is the wave number in the surrounding fluid. Time dependence $\exp(-i\omega t)$ is suppressed. Shear and compressional elastic waves are allowed in the tube wall, and compressional waves are prescribed inside the tube. These are expressed in a form similar to Eq. (3), with one unknown coefficient for the internal wave and two for each component of the elastic wave. Satisfaction of appropriate boundary conditions at the inner and outer shell radii leads to six linear equations with six unknown coefficients. Finally, Cramer's rule is used to find A_m for each value of m, yielding P_{sc}. Three terms were used for all the calculations presented below, which satisfied a convergence criterion of a maximum deviation of 0.1 dB from one mode to the next. Echo level was then calculated with $\mathrm{EL} = 20\log_{10}(P_{\mathrm{sc}}/P_0)$.

3.3 Results

Echo level measurements and the predictions of Eq. (3) are presented in Figure 3. Eq. (3) is for plane wave excitation, but the source did not generate plane waves. To

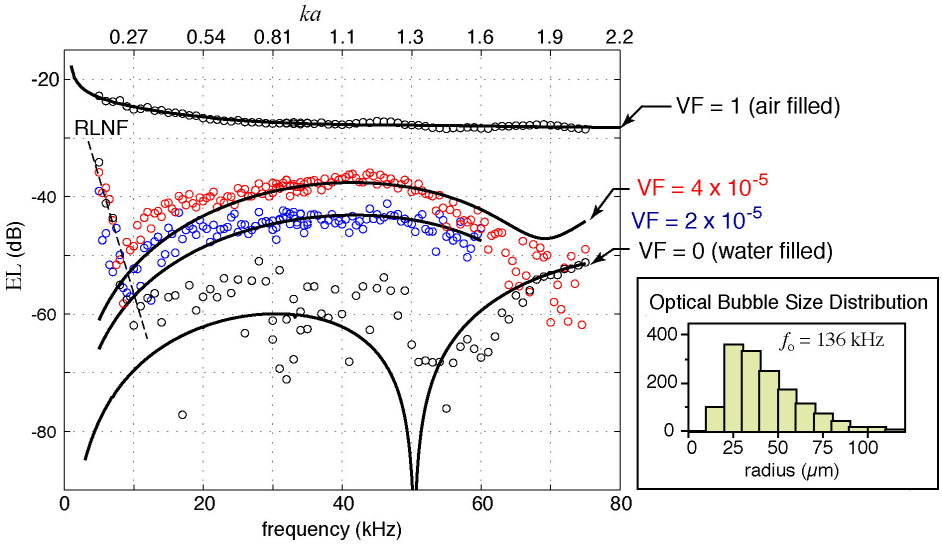

Figure 3. Measured (open circles) and predicted (solid lines) echo levels for a bubbly-liquid-filled tube with outer radius a = 6.4 mm, and inner radius = 4.8 mm. The BSD obtained by photographic analysis is shown in the inset. The frequency associated with the histogram peak is f_0.

account for this frequency-dependent geometric effect, the echo level of a reference target was used for calibration. The air-filled tube (VF = 1 in Figure 3) served as the reference target. The geometric effect will be modeled from first principles in future work. No additional fitted parameters were used for the water-filled case (VF = 0). Best-fit void fractions were obtained for the two intermediate cases. No other adjustable parameters were used.

Good agreement between model and measurement is seen for the two intermediate void fractions between 20 and 60 kHz. A likely cause of greater deviation below 20 kHz is the presence of a bimodal BSD that differed from the one measured in the flow-through imaging chamber. A larger concentration of resonance-size bubbles than shown in Figure 3 could be responsible for the increased echo level. Above 60 kHz, IBRF effects could be invalidating the Wood-limit description of the bubbly liquid.

4 Conclusions

The experiments reviewed in Section 2 support the use of a single-scattering effective medium model [12] to describe the propagation of sound in bubbly liquid with a relatively narrow bubble size distribution, near the individual bubble resonance frequency, up to a void fraction of 5.4×10^{-4}. Knowledge of the bubble size distribution must be an order of magnitude more precise in order to absolutely verify Eq. (1), or any model. The experiments presented in Section 3 support the use of an effective medium model to describe scattering from bubble clouds, at frequencies above the monopole resonance frequency of the cloud, up to ka of order 2, and 55% of the mean bubble resonance frequency.

Acknowledgements

This work was supported by the U.S. Navy Office of Naval Research Ocean Acoustics Program and by Boston University. The authors wish to thank Eun-Joo Park for assistance with measurement and analysis of the BSDs. We also acknowledge our colleague William M. Carey for his insight and guidance during the course of this work.

References

1. Albers V. M., *Underwater Acoustics Handbook II*. (Pennsylvania State University Press, University Park, 1965).
2. Medwin H. and Clay C. S., *Fundamentals of Acoustical Oceanography*. (Academic Press, Boston, 1998).
3. Blanchard D. C. and Woodcock A. H., Bubble formation and modification in the sea and its meteorological significance. *Tellus* **9**, 145–158 (1957).
4. Monahan E. C. and Lu M., Acoustically relevant bubble assemblages and their dependence on meteorological parameters. *IEEE J. Ocean. Eng.* **15**, 340–349 (1990).
5. Thorpe S. A., On the clouds of bubbles formed by breaking wind-waves in deep water, and their role in air–sea gas transfer. *Phil. Trans. R. Soc. Lond.* **A 304**, 155–210 (1982).
6. Thorpe S. A., The effect of Langmuir circulation on the distribution of submerged bubbles caused by breaking wind waves. *J. Fluid Mech.* **142**, 151–170 (1984).
7. Gephart A. D., Acoustic scattering from compact bubble clouds. MS thesis, Boston University, 1999.
8. Roy R. A., Carey W. M., Nicholas M., Schindall J. A., and Crum L. A., Low-frequency scattering from submerged bubble clouds. *J. Acoust. Soc. Am.* **92**, 2993–2996 (1992).
9. Carey W. M. and Browning D., Low frequency ocean ambient noise: Measurements and theory. In *Sea Surface Sound*, ed. by B. R. Kerman (Kluwer, Boston, 1988) pp. 361–376.
10. Karpov S., Prosperetti A., and Ostrovsky L., Nonlinear wave interactions in bubble layers. *J. Acoust. Soc. Am.* **113**, 1304–1316 (2003).
11. Ostrovsky L. A., et al., Nonlinear scattering of acoustic waves by natural and artificially generated subsurface bubble layers in sea. *J. Acoust. Soc. Am.* **113**, 741–749 (2003).
12. Commander K. W. and Prosperetti A., Linear pressure waves in bubbly liquids: Comparison between theory and experiments. *J. Acoust. Soc. Am.* **85**, 732–746 (1989).
13. Feuillade C., The attenuation and dispersion of sound in water containing multiply interacting air bubbles. *J. Acoust. Soc. Am.* **99**, 3412–3430 (1996).
14. Henyey F. S., Corrections to Foldy's effective medium theory for propagation in bubble clouds and other collections of very small scatters. *J. Acoust. Soc. Am.* **105**, 2149–2154 (1999).
15. Wilson P. S., Roy R. A., and Carey W. M., Acoustic scattering from a bubbly-liquid-filled compliant cylinder. *Acoustics Research Letters Online* **2**, 103–108 (2001).
16. Wilson P. S., Roy R. A., and Carey W. M., Phase speed and attenuation in bubbly liquids inferred from impedance measurements near the individual bubble resonance frequency. *J. Acoust. Soc. Am.* **117**, 1895–1910 (2005).
17. Wilson P. S., Roy R. A., and Carey W. M., An improved water-filled impedance tube. *J. Acoust. Soc. Am.* **113**, 3245–3252 (2003).
18. Wood A. B., *A Textbook of Sound*, 1st ed. (MacMillan, New York, 1930).
19. Doolittle R. D. and Überall H., Sound scattering by elastic cylindrical shells. *J. Acoust. Soc. Am.* **39**, 272-275 (1966).